CHARACTERIZATION OF THE CHARGE DISTRIBUTION OF AIRBORNE DUST IN CANADIAN URANIUM AND NON-URANIUM MINES

M. GRENIER May 1988

MINING RESEARCH LABORATORIES
DIVISION REPORT MRL 88-66 (OPJ)

Published in the American Industrial Hygiene Association Journal; Volume 50; #8, pps 383-390, August 1989.

SUMMARY

The levels of charge found on airborne dust from various mining and milling operations were measured. More specifically, uranium and non-uranium operations were surveyed and definite differences in charge distribution were observed. Charge distributions in both types of mines were noted to be symmetrical (net neutral), and while data from non-uranium mines and mills showed good agreement with data gathered by other investigators, uranium mine and mill results seemed to be abnormally low for the types of operations involved. For example, the number of elementary charges associated with 7.5 μm dust was 24 for uranium mines compared with 197 for non-uranium mines at underground primary crusher operations. Similar differences were noted at surface secondary crushing plants where the number of charges measured were 15 and 71, respectively, for uranium and non-uranium mills, again for 7.5 μm dust. In an effort to explain these differences, the effect of the level of mechanization, relative humidity and the airborne concentration of neutralizing free-ions is discussed.

Characterization of the charge distribution of airborne dust in Canadian uranium and non-uranium mines.

Michel G. Grenier

Research Scientist, Elliot Lake Laboratory, CANMET,
Energy, Mines and Resources Canada, Elliot Lake, Ontario, Canada, P5A 2J6

INTRODUCTION

Airborne dusts and aerosols are known to carry a number of positive and negative charges.[1] The amount of charge on particles usually lies between a lower and an upper limit. The lower limit is generally recognized to follow the Boltzmann distribution law. In time, most dust clouds through interaction with airborne free ions will discharge until Boltzmann equilibrium is reached (Figure 1). The Rayleigh limit which is normally used as an upper limit value refers to the maximum number of charges that a given size water droplet may carry before mechanical instability is reached. The Rayleigh limit shown in Figure 1 is rarely exceeded in practice. Charge distributions in most industrial environments are likely to be found in the range defined by the graph shown in Figure 1.

Accumulated electric charges on dust particles have long been suspected of enhancing lung deposition. Recent work[2] confirms this and shows that there exists a threshold charge level dependent on particle size, which when exceeded enhances alveolar deposition by the induction of image charges on nearby lung tissue. The assessment of airborne dust charge distribution is also important as the performance of dust samplers may be affected by excess charge carried by dust particles. These effects are not negligible and are especially noticeable in samplers made from non-conductive materials.[3,4]

The charging of dust to levels well above the Boltzmann limit is achieved under a variety of situations. In the laboratory, dust dispensers and aerosol generators are known to produce highly charged particles which must usually be conditioned by an aerosol neutralizer. During these operations, charges are carried off by particles upon leaving the dispenser or induced when liquids are atomized.

In industry, charging of dust to levels beyond the Boltzmann

equilibrium arises from heavy duty mechanical processes such as crushing. grinding and bulk materials handling and transportation. In some cases. the resulting charged dust cloud is said to be symmetrical or net neutral with a similar number of positive and negative dust particles. Most of the work performed at mine plants has shown that in the majority of cases dust clouds are at. or very close to. electroneutrality.(1)

Whereas the breaking of bonds and the sudden separation of materials leads to the formation of charged airborne dust. there are several mechanisms that will tend to neutralize dust to levels close to the Boltzmann equilibrium limit. Unless the process responsible for the high charge level is kept up. charges on airborne dust particles will be reduced by the capture of free ions. Free ions are charged gas molecules found at varying concentrations in air. Typically, they arise as a result of ion pair production from cosmic radiation and other radioactive decay schemes. Small bipolar ions may also be produced by corona discharge. These free ions are present in positive and negative form and thus will recombine. The rate of production of free ions and the rate of recombination will lead to an equilibrium free ion density which will depend on the relative importance of the two phenomena. Typical concentrations of free ions in clean country air are likely to be less than 5.000 ions/cm^3 (5). and theoretical calculations suggest that in some working environments this value may be as high as 40.000 ions/cm^3 or more.(6)

Knowing that the level of charge on airborne dust may potentially affect lung deposition and/or dust sampler performance. the aim of this project was to establish the charge distribution of airborne dust at several surface and underground operations in uranium and non-uranium mines. Data were then compared amongst themselves and to results from similar studies conducted elsewhere.

METHODS AND INSTRUMENTS

The charge distribution of dust was measured with the help of a split-flow elutriator (SFE) designed by the staff of the Physics Branch of the Edinburgh Institute of Occupational Medicine.[7] This instrument when used in conjunction with a size discriminating dust monitor is able to simultaneously measure the electrical mobility and hence the number of elementary charges associated with dust in several size ranges. The SFE is not available on the market and was duplicated at the Elliot Lake Mining Research Laboratory for the purpose of this study. Two SFEs were built and an evaluation of the units was performed. These tests showed that the instruments perform well and are rugged enough to sample under harsh field conditions.[8]

The SFE consists of a rectangular channel lined with two oppositely charged conducting plates. Air enters the channel and travels the length of the elutriator before exiting via the flow splitting end cap. The design of this end cap enables the apparatus to be used in one of two working configurations. One of these is termed the B($\pm$) configuration and is used to establish the charge distribution while discriminating between positively and negatively charged dust particles. This configuration is usually used when sampling an area or process for the first time. If it is found that the dust cloud is symmetrical (neutral), then the apparatus is used in the A configuration. The experimental procedure and the data analysis in this configuration is far simpler. In all of the tests that were performed here, the results of B($\pm$) runs have shown the dust clouds to be net neutral and the data reported are the result of type A runs.

The SFE is used with an external power supply (EG & G model 459, EG & G Ortec, Oak Ridge, TN. USA), and a Mono Research Ltd. (Brantford. Ontario. Canada) optical counter (modified HIAC/ROYCO model 4100). The apparatus in a

type A configuration is shown in Figure 2. In a typical sampling run. the voltage supplied to the SFE plates is varied in steps between 0 and 5000 VDC. As the voltage is increased more of the charged particles are removed by attraction to the plates and particle mobilities may be deduced by analyzing the output concentration as a function of the applied voltage. Finally, the charge characteristics are examined simultaneously in six preset size ranges with the help of the modified optical dust counter. This allows the charge distribution or the number of elementary charges as a function of size to be determined. The specifics of sampling and data analysis are given in detail elsewhere.[7,8]

In the course of this study. charge distributions were measured in uranium and nickel mines. Processes surveyed included surface milling operations such as ore transport. ore grinding, and secondary crushing as well as underground mining operations such as loading and hauling of ore at work headings and primary crushing. Upon arrival on site. the equipment was assembled and started. The actual determination of charge distribution was made during dust producing operations when dust concentration in all size ranges was constant as measured by the optical particle counters.

RESULTS

Results from the survey are shown in Table I and Figures 3 to 6. These Figures show the median number of elementary charges as a function of dust particle size for all tests conducted. Table I lists power curves fitted to data from every experiment. The power curve is in the form:

$$q_m = Kd^n \qquad \text{Eq 1}$$

where, q_m is the median number of elementary charges per particle.

d is the particle diameter. (μm).

K is the median number of charges carried by a 1 μm dust particle.

Tests 1 to 3 were conducted in a nickel mining operation. These data are also shown graphically in Figure 3 along with the Boltzmann equilibrium lower limit. Test 1 was performed at a secondary crushing operation in a surface mill. Tests 2 and 3 were conducted, respectively, underground at a primary crushing station, and in a work heading where blasted ore was being loaded and hauled by a diesel scooptram. Results from tests 1 to 3 and Figure 3 show high positive correlation in the power curve fitting procedure. The average median number of charges for 1 μm diameter dust is 4.3 (K), and the power index (n) is 1.7. Primary crushing was observed to yield higher levels of charge than secondary crushing. This is consistent with data from tests performed elsewhere.[1]

Tests 4 to 8 were conducted in uranium mines. Tests 4 to 7 were performed on surface at different stages of the milling process. Test 4 was conducted close to a belt conveyor transporting coarse ore recently brought up from underground and dumping it into an ore bin. In test 5, sampling took place at a secondary crushing plant. Test 6 was performed close to a semi-autogenous ore grinding operation, and test 7 next to a disc filter used to remove water from ground pulp. Test 8 was carried out underground at a primary crushing operation. These data are shown graphically in Figure 4.

From Table I it appears that all uranium mill tests show high positive correlation. The underground primary crusher test (test 8), however, shows a correlation coefficient of 0.77, which on 5 points is not considered high enough to show positive correlation. Tests on the underground crushing platform were repeated several times with similar results being obtained. The reason for this lack of agreement to a power fit cannot be explained at this time.

If test 8 is omitted in the calculation of an average K coefficient, we obtain a value of 2.0 elementary charges. This is approximately half of that

calculated for nickel operations. Similarly, the power index (n) is 0.90, or also approximately half of the index calculated for nickel mines. From Figure 4, it is noticed that slopes are fairly similar and that highly mechanized processes such as primary and secondary crushing show a large median number of charges compared to other milling processes. Finally, the charge distributions obtained in uranium operations are unexpectedly low and close to the Boltzmann equilibrium limit. Data from other investigators[1] and the work performed here in nickel mines show numbers of elementary charges that are up to one order of magnitude higher than those measured at comparable uranium operations. This is especially noticeable for larger diameter dust and is reflected in the graphs of Figures 5 and 6.

Figure 5 shows data from primary crushing operations. On this graph, the Boltzmann lower limit is shown as well as the results from three field tests. Tests 2 and 8 (nickel and uranium) are compared with data from a primary crushing operation in a U.K. quarry. Data collection and analysis in the U.K. tests were performed with similar instruments and using similar techniques.[1] These data are added for the sake of comparison and should not be analyzed in much depth as little information is available on the nature of the crushed material and crushing apparatus. When comparing tests 2 and 8, however, it can be seen that although differences for smaller diameter dust are minimal, median number of charges in the 4 to 10 μm range are 5 to 10 times higher at nickel primary crushing operations. This is also evident from secondary crushing data shown in Figure 6. Data from the U.K. quarry secondary crusher, and those from the nickel mill are identical while uranium mill results are systematically lower.

DISCUSSION

From data given in the previous section it is clear that uranium mine operations have dust charge distributions that are very low for the type of work being conducted. And while similarities between nickel mine crushing operations and crushing in the U.K. quarries may be fortuitous. some explanations are needed for uranium mine and mill data. Several factors come to mind which could be at the root of these differences. Among these. are the level of mechanization influenced by the type and size of crusher used. differences in temperature or relative humidity. and differences in airborne concentration of bipolar free ions. Each of these factors will be discussed in detail in this section. In doing so, only the data from crushing operations (primary and secondary) will be used.

Level of Mechanization and Relative Humidity

Table II lists a few parameters describing environmental conditions and crusher types and specifications. As far as primary crushing is concerned both mining companies used Traylor jaw type crushers. The jaw is 90 cm wide by 120 cm deep, and the minimum jaw gap is set at 13 cm, although with time the jaw may be allowed to wear to 18 cm. The crushers are operated in conjunction with 150 H.P. motors. In secondary crushing operations. both mills use cone type crushers which are specified mainly by cone diameter and gap set. In the nickel mill, Allis Chalmers crushers with 210 cm diameter cones at the base, and a 1.3 to 2.5 cm gap set. were used. Uranium mines used Rexnord crushers equipped with 170 cm cones with a gap set of approximately 1 cm.

From these figures it seems that the level of mechanization is fairly similar at both operations. Indeed, primary crushers are identical in process and specifications, while the secondary crushers are of the same type with

minor differences in cone diameters and gap sets. It seems unlikely, therefore, that the difference in charge distribution is caused by differences in processing.

Examination of relative humidity data from Table II shows that for primary crushing, at least, conditions were similar at both operations. Other studies have also shown that variations in airborne dust charge levels could not be attributed to the effect of air moisture content in environments where relative humidity varied between 40 and 90%.[1]

Concentration of Airborne Free Ions

In this section, the possibility of an excess of free ion concentration present in uranium mines is examined. It is conceivable, given the radioactive nature of the ore found in uranium mines that radon and thoron gas emanations lead to high levels of free ions formed by the decay in air of these gases and their progenies. This excess in free ion concentration in turn would lead to an accelerated rate of neutralization of charged dust in uranium mine operations. We will concentrate on underground primary crusher data in this section of the discussion.

A few assumptions have to be made, the first of which consists in accepting that the initial amount of charge produced at both the uranium and the nickel ore crushers are similar. In other words, immediately after the rock is crushed, and before free ions have a chance to begin the neutralization process, we assume that both dust clouds are similarly charged. This is not unreasonable given the fact that both operations involve identical jaw crushers. We will further assume that the time required for the dust produced to travel from the point of production to the point of sampling is the same at both crusher locations. Measurements indicate residence times of 40 to 60 seconds in both cases. Finally, we will assume that radioactive

contaminants concentration gradients (and hence. free ion concentration gradients) do not exist between the point of dust production and the sampling area. This is not likely to be the case and the effect of such gradients will be discussed later.

In 1974. Liu et al.[9] developed and verified the following equation. which applies to the neutralization of airborne charged dust:

$$Nt = \frac{1}{4\pi Ze} \ln\left(\frac{n_i}{n_f}\right) \qquad \text{Eq 2}$$

where, t is the exposure time of dust to discharging bipolar ions (sec).

n_i is the initial number of elementary units of charge per dust particle.

n_f is the final number of elementary units of charge per dust particle after time t.

e is the elementary unit of charge (4.8×10^{-10} statcoulomb)

Z is the ion mobility (cm^2/statV sec),

N is the free ion concentration for either polarity (ions/cm^3).

The above equation is valid for the continuum regime where particle radii are much larger than the mean free path of ions. It was developed mainly to predict the level of neutralization of charged particles in the simple geometry of laboratory neutralizing tubes. Such tubes have the inside wall coated with a radioactive substance which produces high concentrations of ion pairs that neutralize charges on dust and aerosols passing by.

If equation 2 is applied to the case of the uranium and nickel mines separately, we obtain equations 3a and 3b:

$$N_u t = \frac{1}{4\pi Ze} \ln\left(\frac{n_i}{n_{fu}}\right) \qquad \text{Eq 3a}$$

$$N_{ni} t = \frac{1}{4\pi Ze} \ln\left(\frac{n_i}{n_{fni}}\right) \qquad \text{Eq 3b}$$

where the subscripts u and ni refer to the case of uranium and nickel mines.

respectively, and Z in the equations is defined by:

$$Z = \frac{De}{kT} \qquad \text{Eq 4}$$

where. D is the diffusion coefficient of free ions (3×10^{-2} cm^2/sec),

k is Boltzmann's constant (1.38×10^{-16} $erg/^oK$),

T is the absolute temperature (^oK).

Subtracting 3b from 3a and substituting Z and known constants we obtain:

$$N_u - N_{ni} = \frac{4.66 \times 10^5}{t} \ln\left(\frac{n_{fni}}{n_{fu}}\right) \qquad \text{Eq 5}$$

Equation 5 may be used to estimate the excess free ion concentration ($N_u - N_{ni}$) required to explain the difference in airborne dust charge level after a given residence time t. Data for n_{fni} and n_{fu} were obtained from the graph shown in Figure 3. and $N_u - N_{ni}$ was evaluated for times t ranging between 10 and 200 sec. The ion pair concentration difference thought to be caused by airborne radioactivity is shown graphically in Figure 7 for 3. 5 and 10 μm dust.

The dust concentration as a function of time measured by the optical dust counter showed that the dust concentration in both instances decreased rapidly after crushing had ceased. with clearing times between 40 to 60 sec. If we accept a value of 50 sec as an approximation for t, we note that $N_u - N_{ni}$ lies in a range between 10,000 and 23,000 ion pairs/cm^3. This range compares favourable with an estimate of ion pair concentration due to radioactive decay products in a uranium mine. This estimate[6] assumes that α-decay from radon gas and short-lived decay products is the largest contributor to ion-pair formation. This analysis yields a value of approximately 22,000 ion pairs/cm^3 for 100 pCi/L of radon in equilibrium with its decay products. In reality. radon gas concentrations in the uranium ore crushing plant surveyed here are closer to 60 pCi/L and equilibrium with decay products is rarely reached. Typical activities for daughters Po-218 and Po-

214 are 33 and 10 pCi/L, respectively. These values are an average calculated from previously collected data on the crushing platform. Following the above treatment.[6] the ion pair concentration due to α-decay of radon and its products comes to 13,000 ion-pairs/cm^3. This does not take into account α-decay from thoron and its progeny, which are common occurrences in these mines.

Concentration Gradients of Airborne Free Ions

The preceding section made the assumption that the concentration of decay products, and hence that of free ions in air, between the crushing point and the sampling area was constant. This assumption is not a strictly valid one to make in an underground environment where radon trapped in the ore is suddenly released during the crushing process. This applies even more in a surface environment such as the uranium ore secondary crushing plant. The airborne decay product concentrations measured in this plant are not high enough to explain the difference in charge observed between nickel and uranium operations.

In an attempt to explain the difference, an estimate was made of the amount of radon spontaneously released when crushing uranium ore. Although no previous work could be found for the case of primary crushers, some laboratory work had been done which could be related to the case of secondary crushers. In this work[10], the authors experimentally measured the amount of radon released per unit mass of ore crushed to less than 2 cm in diameter. This is very similar in size to the gap set of the uranium mill primary crusher (1 cm). The authors in this case found that 115 pCi of radon were released per gram of ore with a grade of 2.1 kg of uranium per tonne. In the case of interest here, the ore grade was 0.82 kg/tonne, which, if we compare with literature data will result in the release of at least 45 pCi/gram if we

assume similar host rock properties. The uranium crushers have an average feed rate of 185 tonnes/h, or 52,000 g/sec. Therefore, the potential exists for 2.3×10^5 pCi of radon to be released during every second of the process. This amount of radon (not including decay products) in one litre of air can potentially create 2×10^6 ion pairs/cm^3. It is, therefore, apparent that a free ion concentration gradient is likely to exist in uranium underground and surface crushing operations. It is possible then, that a major portion of the neutralization process occurs very rapidly, soon after the uranium ore is crushed.

CONCLUSION AND FUTURE RESEARCH

It was observed that a marked difference exists between charge distributions measured at similar operations in uranium and non-uranium mines. Data from non-uranium operations are in close agreement with data gathered at similar operations by other investigators. This and low results observed at uranium ore processing plants seem to indicate that there are mechanisms at work in uranium mines and mills that tend to neutralize charged dust. One likely explanation was presented that suggests that an excess concentration of airborne free ions is present in uranium plants. No direct experimental data was offered to support the preceding hypothesis: these were advanced solely for the purpose of discussion. Proper field and laboratory tests will be required to shed some light on the subject.

It is suggested that laboratory experiments be conducted on two fronts. First, the amount of radon released per gram of local crushed ore should be determined. Second, the crushing of uranium and nickel (or non-uranium) ores could be performed in the laboratory, and charge distributions of the dust produced could be analyzed in a laboratory chamber. Field tests are also required to measure the amount and distribution of free bipolar ions in the

vicinity of mechanized operations in uranium and non-uranium mines and mills.

ACKNOWLEDGEMENT

The author would like to thank K. Butler for technical assistance, and J. Bigu for the advice provided. The advice and encouragement extended by A.M. Johnston and J.H. Vincent of the Edinburgh Institute of Occupational Medicine was greatly appreciated. Finally, the staff of Rio Algom Ltd., Elliot Lake Operations, and Falconbridge Ltd., Sudbury Operations are to be commended for their diligence and kind help.

REFERENCES

1. Johnston, A.M., J.H. Vincent and A.D. Jones: Measurement of Electric Charge for Workplace Aerosols. Ann. Occup. Hyg. 29(2):271-284 (1985).
2. Prodi, V. and A. Mularoni: Electrostatic Lung Deposition Experiments with Humans and Animals. Ann. Occup. Hyg. 29(2):229-240 (1985).
3. Liu, B.Y.H., D.Y.H Pui, K.L. Rubow and W.W. Szymanski: Electrostatic Effects in Aerosol Sampling and Filtration. Ann. Occup. Hyg. 29(2): 251-269 (1985).
4. Blackford, D.B., G.W. Harris and G. Revell: The Reduction of Dust Losses within the Cassette of the Simpeds Personal Dust Sampler. Ann. Occup. Hyg. 29(2):169-180 (1985).
5. Gunn, R.: Diffusion Charging of Atmospheric Droplets by Ions, and the Resulting Combination Coefficients. J. Meteorol. 11(5):339-347 (1954).
6. CANMET, Energy, Mines and Resources Canada: On the Potential Biological Influence of Small Ions on Personnel Working in Underground Uranium Mine Atmospheres, by J. Bigu. Division Report MRP/MRL 80-62(TR). Elliot Lake, Ontario, Canada: CANMET, Energy, Mines and Resources Canada, 1980.
7. Johnston, A.M.: A Semi-Automatic Method for the Assessment of Electric

Charge Carried by Airborne Dust. Ann. Occup. Hyg. 14(5):643-655 (1983).

8. CANMET, Energy, Mines and Resources Canada: Evaluation of a Split-Flow Elutriator Used in the Determination of Airborne Dust Charge Distributions, by M.G. Grenier and K. Butler. Division Report MRL 87-187 (TR). Elliot Lake, Ontario, Canada: CANMET, Energy, Mines and Resources Canada, 1987.

9. Liu, B.Y.H. and D.Y.H. Pui: Electrical Neutralization of Aerosols. J. Aerosol Sci. 5:465-472 (1974).

10. Macek, J. and F. Strehovec: "Radon-222 Releases from Crushing, Grinding and Leaching of Uranium Ore". IAEA-SM-217/42 Int. Symp. on the Monitoring of Radioactive Airborne and Liquid Releases from Nuclear Facilities. Ljubljana, Yugoslavia, September 5-9. 1977.

TABLE I

Power Curve Regression of Charge Distribution Data from Field Tests

Test	Operation (Mine)	K	n	Correlation Coefficient (r^2)
1	Secondary Crusher (nickel)	3.4	1.53	0.99
2	Primary Crusher (nickel)	4.0	2.02	0.99
3	Ore Transport (nickel)	5.5	1.56	0.99
4	Belt Conveyor (uranium)	2.0	0.84	1.00
5	Secondary Crusher (uranium)	1.9	1.05	1.00
6	Ore Grinder (uranium)	1.6	1.00	1.00
7	Disc Filter (uranium)	2.3	0.70	0.95
8	Primary Crusher (uranium)	5.7	0.79	0.77

TABLE I1

Crusher Specifications and Environmental Conditions

Test	Crushing Operation	Type	Dimensions (cm)	RH (%)	T (^{o}C)
2	Primary (nickel)	Jaw	90 W x 48 D x 13 gap	72	26
8	Primary (uranium)	Jaw	90 W x 48 D x 13 gap	82	18
1	Secondary (nickel)	Cone	210 dia. x 1.3-2.5 gap	35	22
5	Secondary (uranium)	Cone	170 dia. x 1.0 Gap	--	--

FIGURE CAPTIONS

Figure 1 -- Theoretical lower (Boltzmann) and upper (Rayleigh) limit of electrical charge on particles.

Figure 2 -- Charge distribution sampling apparatus consisting of a power supply, the split-flow elutriator (SFE), an optical particle counter (OPC) and data logging devices.

Figure 3 -- Charge distributions from various nickel mine and mill operations.

Figure 4 -- Charge distributions from various uranium mine and mill operations.

Figure 5 -- Charge distributions from primary crushing operations.

Figure 6 -- Charge distributions from secondary crushing operations.

Figure 7 -- Theoretical free ion concentration difference between uranium and nickel underground mine atmospheres.

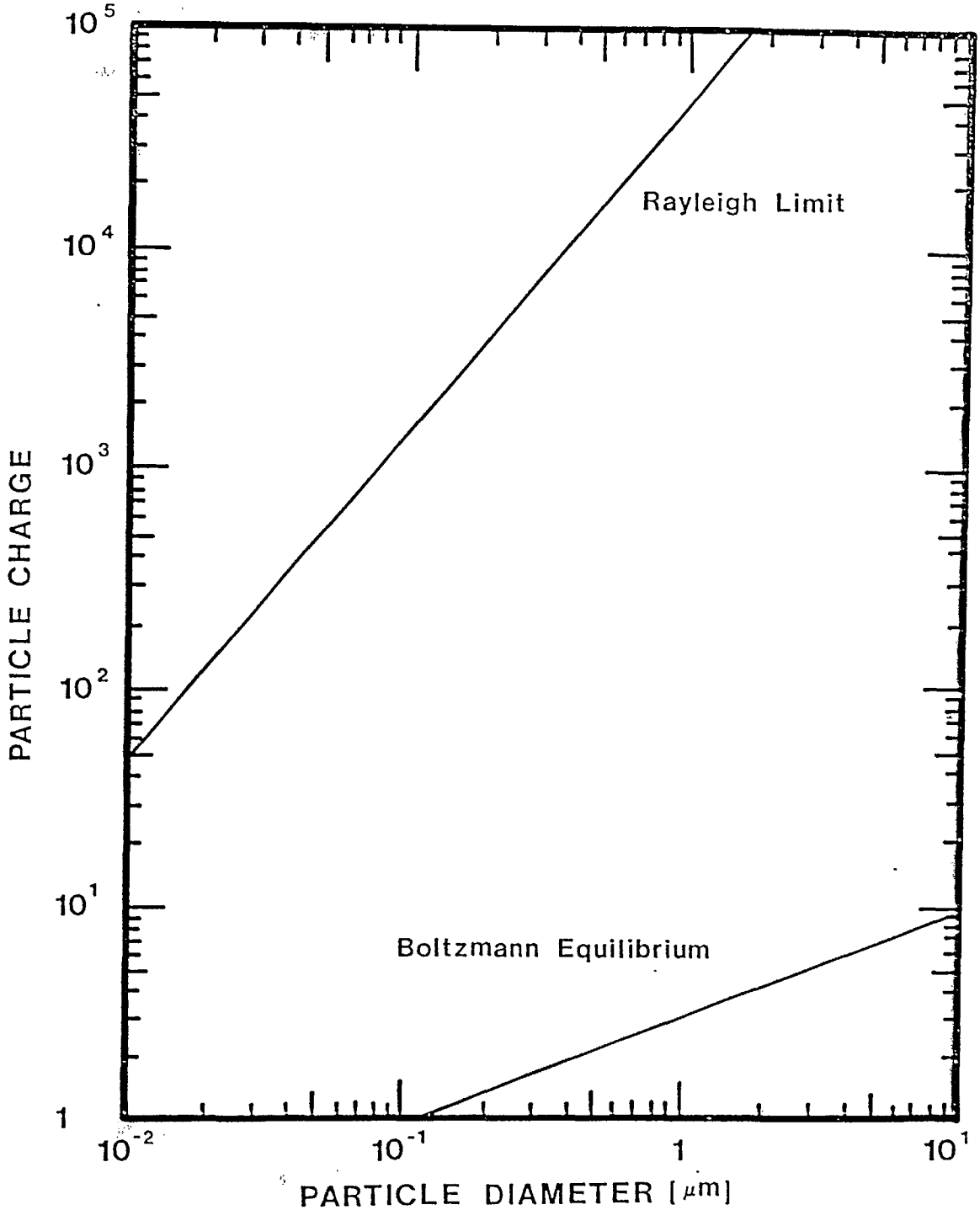
10^5
10^4
10^3
10^2
10^1
1
PARTICLE CHARGE
Rayleigh Limit
Boltzmann Equilibrium
10^{-2}
10^{-1}
1
10^1
PARTICLE DIAMETER [μm]

Figure 1

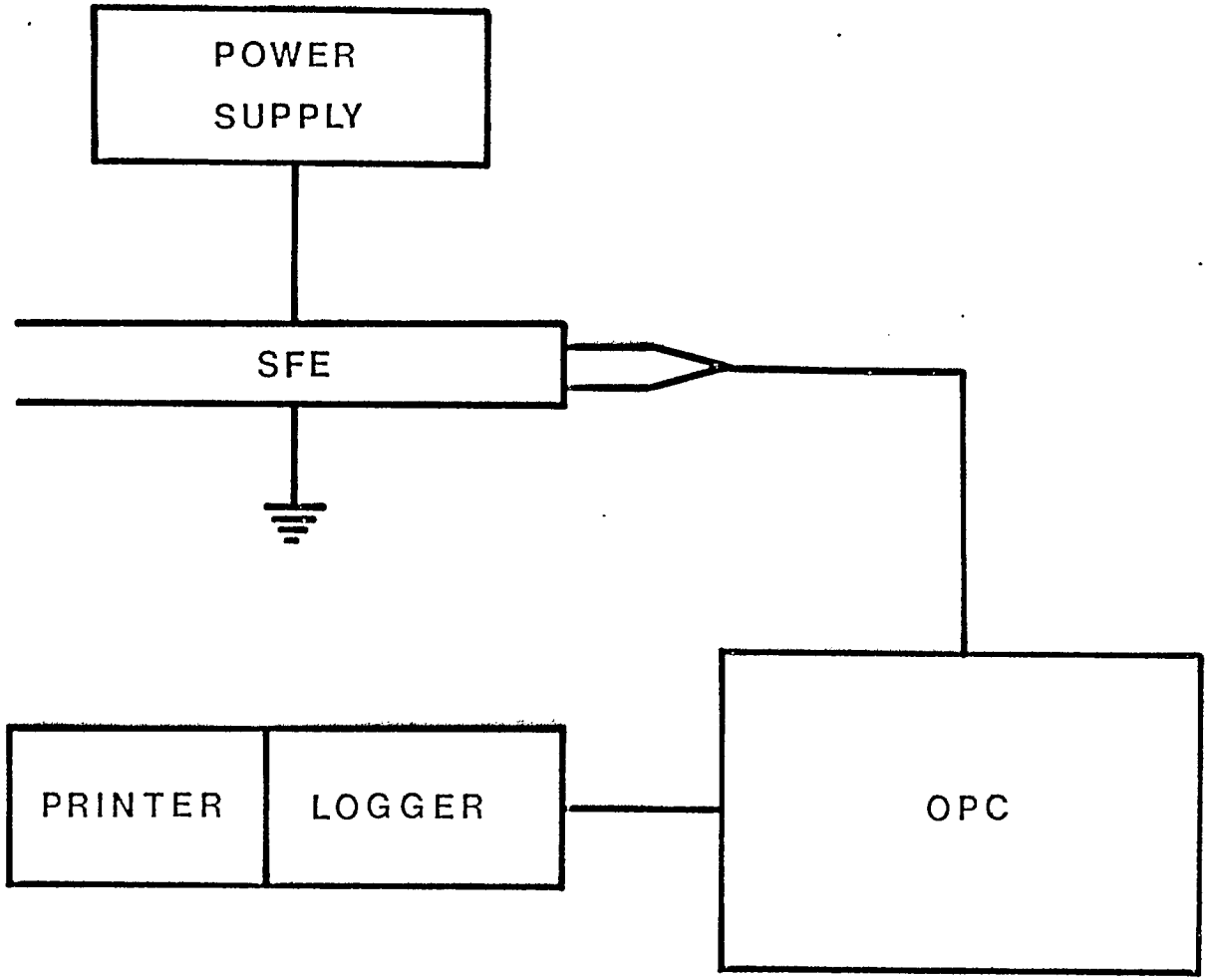

Figure 2

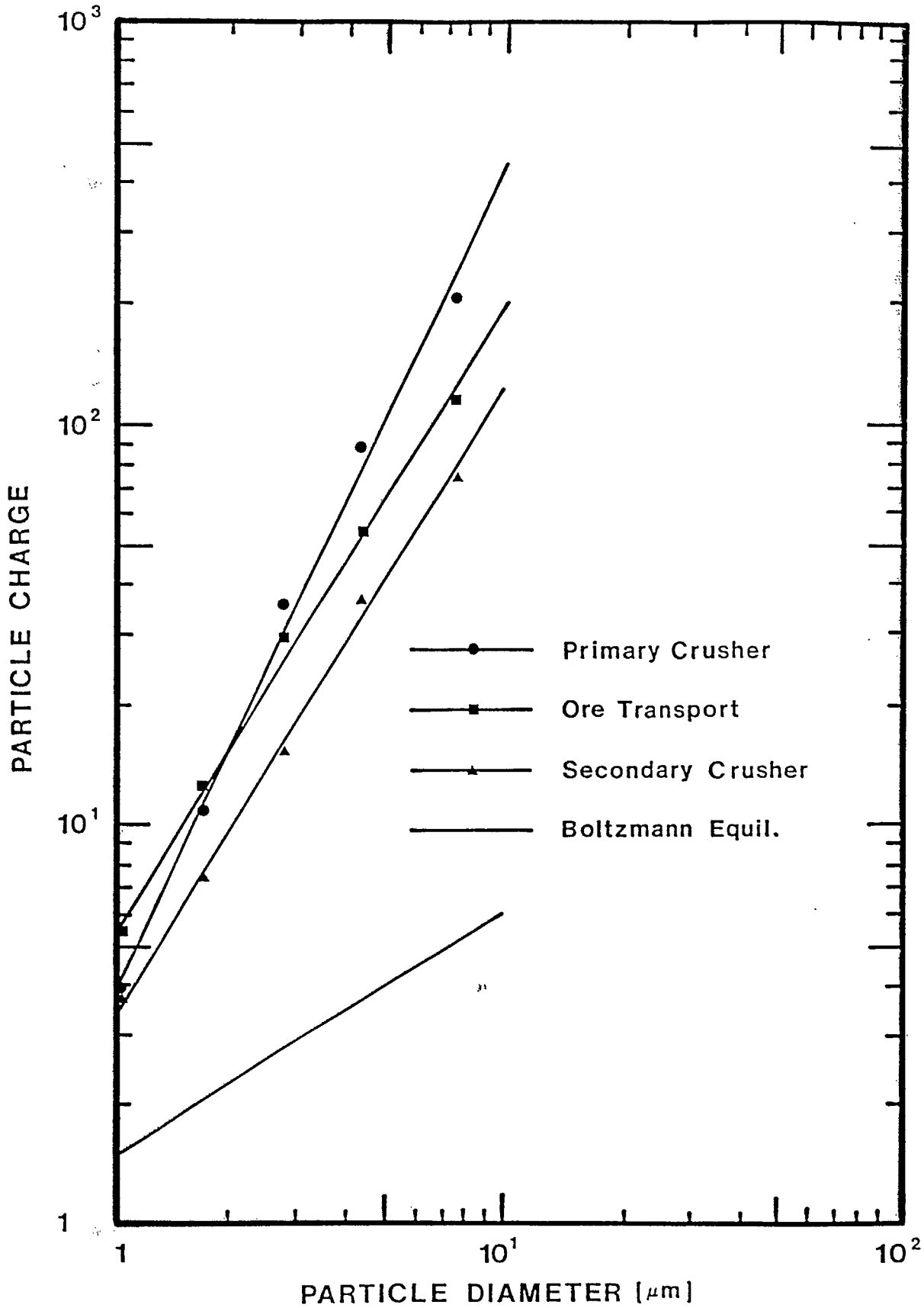
10^3
10^2
10^1
1
PARTICLE CHARGE
1
10^1
10^2
PARTICLE DIAMETER [μm]
Primary Crusher
Ore Transport
Secondary Crusher
Boltzmann Equil.

Figure 3

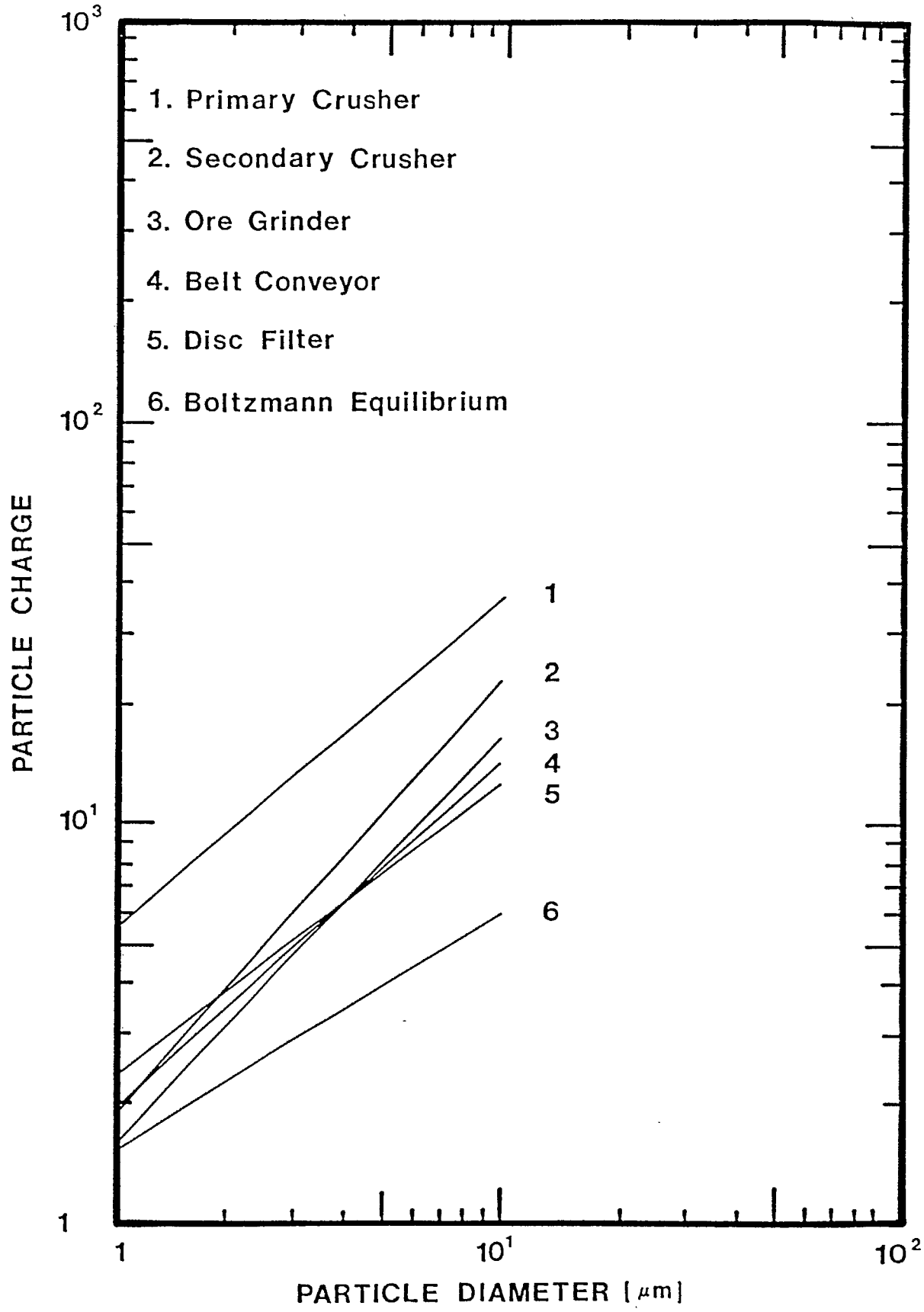
1. Primary Crusher
2. Secondary Crusher
3. Ore Grinder
4. Belt Conveyor
5. Disc Filter
6. Boltzmann Equilibrium
PARTICLE CHARGE
PARTICLE DIAMETER [μm]
10^3
10^2
10^1
1
1
10^1
10^2
1
2
3
4
5
6

Figure 4

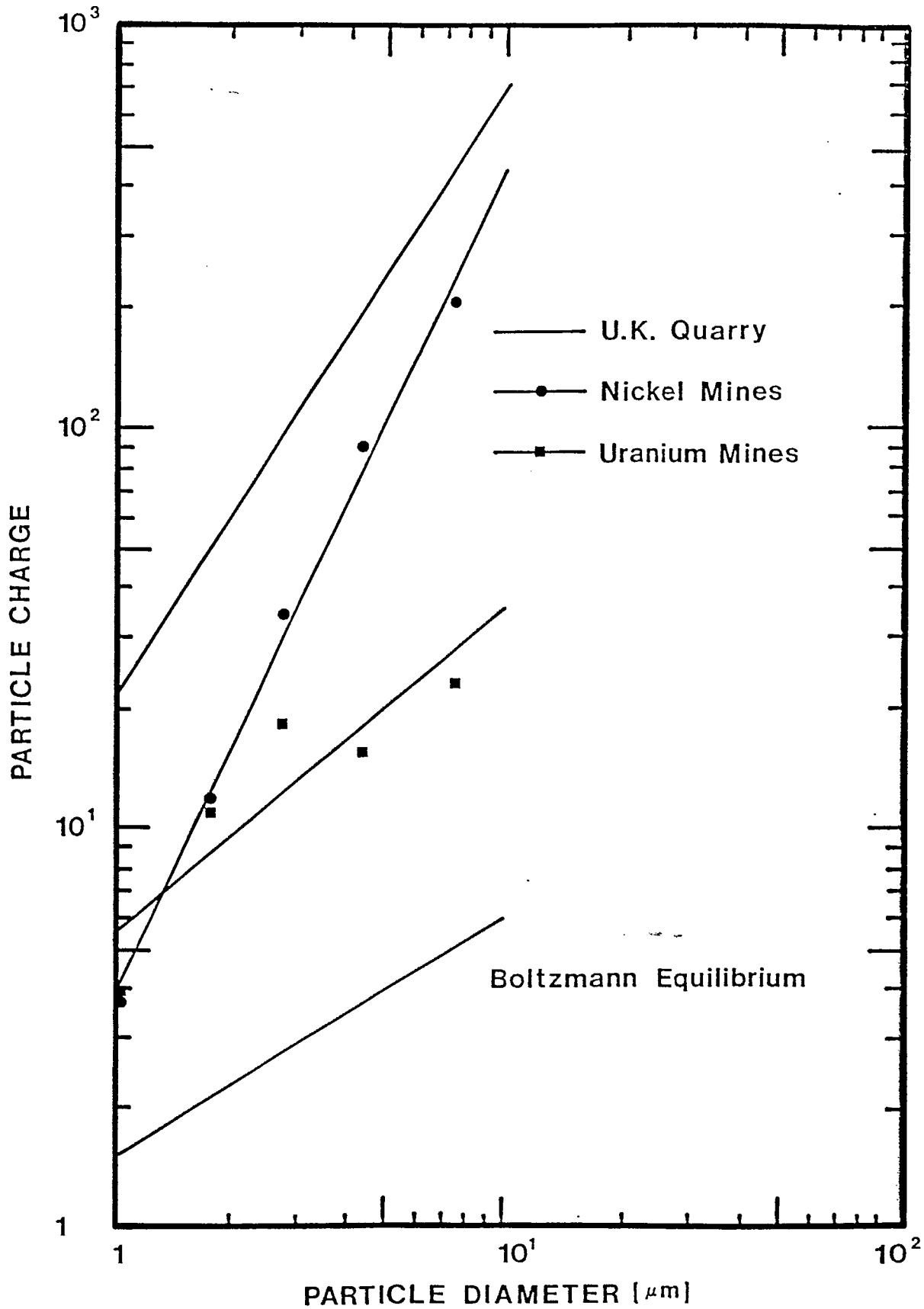
10^3
10^2
10^1
1
PARTICLE CHARGE
U.K. Quarry
Nickel Mines
Uranium Mines
Boltzmann Equilibrium
1
10^1
10^2
PARTICLE DIAMETER [μm]

Figure 5

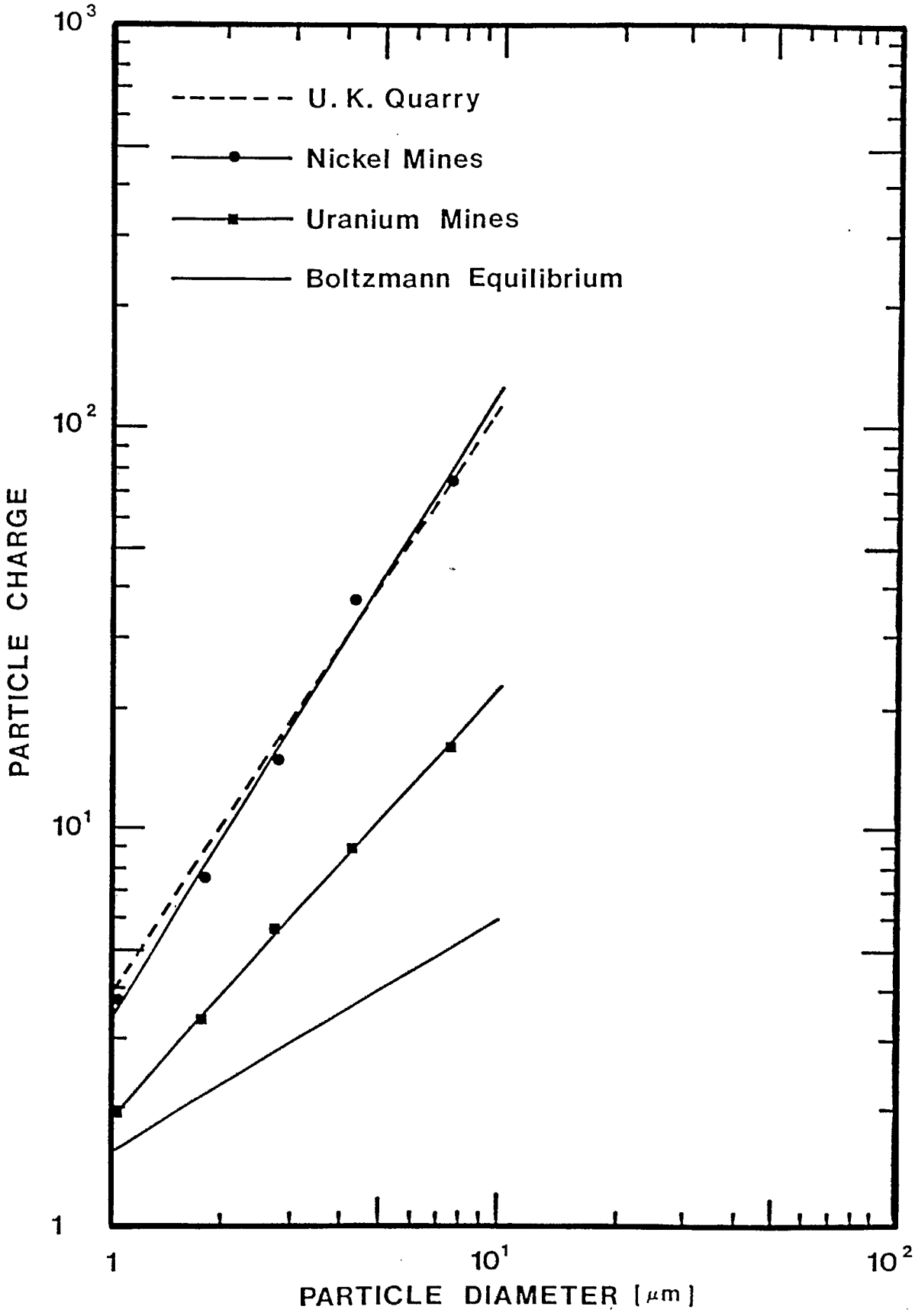
U. K. Quarry
Nickel Mines
Uranium Mines
Boltzmann Equilibrium
PARTICLE CHARGE
PARTICLE DIAMETER [μm]
10³
10²
10¹
1
1
10¹
10²

Figure 6

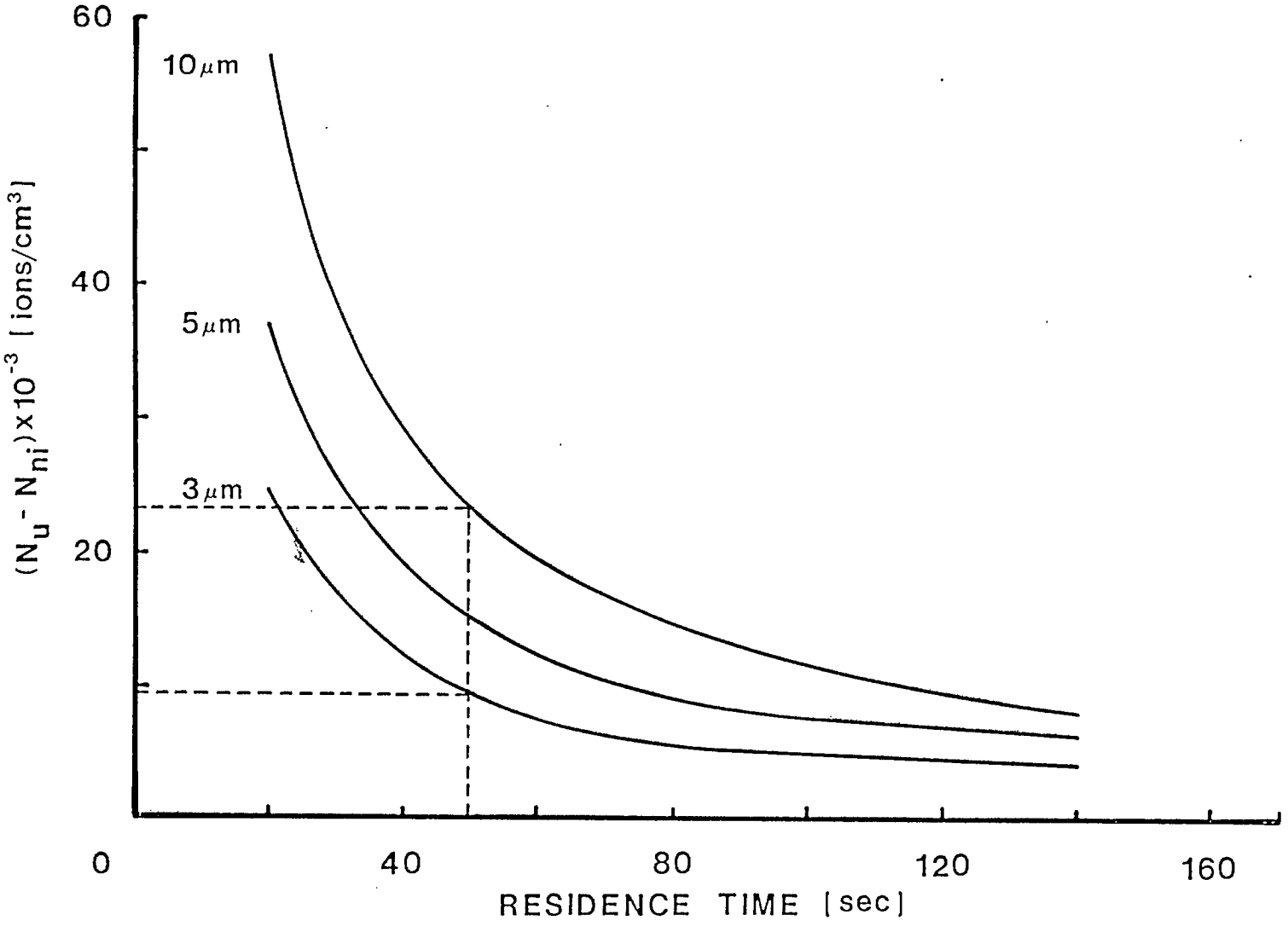
60
40
20
0
10μm
5μm
3μm
$(N_u - N_{ni}) \times 10^{-3}$ [ions/cm^3]
40
80
120
160
RESIDENCE TIME [sec]

Figure 7